AFRL-AFOSR-VA-TR-2019-0278

Nanoelectropulse-induced changes in cell excitability - a new approach for neuromodulation

Gale Craviso
UNIVERSITY OF NEVADA RENO

09/12/2019
Final Report

Air Force Research Laboratory
AF Office Of Scientific Research (AFOSR)/ RTB2
Arlington, Virginia 22203
Air Force Materiel Command

DISTRIBUTION A: Distribution approved for public release.

REPORT DOCUMENTATION PAGE

Form Approved
OMB No. 0704-0188

1. REPORT DATE *(DD-MM-YYYY)*	2. REPORT TYPE	3. DATES COVERED *(From - To)*
23-09-2019	Final Performance	15 Jun 2014 to 14 Jun 2019

4. TITLE AND SUBTITLE
Nanoelectropulse-induced changes in cell excitability - a new approach for neuromodulation

5a. CONTRACT NUMBER

5b. GRANT NUMBER
FA9550-14-1-0018

5c. PROGRAM ELEMENT NUMBER
61102F

6. AUTHOR(S)
Gale Craviso

5d. PROJECT NUMBER

5e. TASK NUMBER

5f. WORK UNIT NUMBER

7. PERFORMING ORGANIZATION NAME(S) AND ADDRESS(ES)
UNIVERSITY OF NEVADA RENO
204 ROSS HALL MS 325
RENO, NV 89557 US

8. PERFORMING ORGANIZATION REPORT NUMBER

9. SPONSORING/MONITORING AGENCY NAME(S) AND ADDRESS(ES)
AF Office of Scientific Research
875 N. Randolph St. Room 3112
Arlington, VA 22203

10. SPONSOR/MONITOR'S ACRONYM(S)
AFRL/AFOSR RTB2

11. SPONSOR/MONITOR'S REPORT NUMBER(S)
AFRL-AFOSR-VA-TR-2019-0278

12. DISTRIBUTION/AVAILABILITY STATEMENT
A DISTRIBUTION UNLIMITED: PB Public Release

13. SUPPLEMENTARY NOTES

14. ABSTRACT
This multidisciplinary project has been to explore the potential for nanosecond-duration electric pulses (NEPs) to serve as a safe and potentially non-invasive approach for altering neural cell excitability, with the overall objective of developing new ways to enhance human performance. Our strategy combined experimental and computational approaches to elucidate how very short duration (less than 10 ns in duration) electric pulses of high intensity (>1 megavolt-per-meter; MV/m) alter the excitability of isolated bovine adrenal chromaffin cells, a leading non-transformed model of neurosecretion. Crucial to the success of the project was designing and fabricating a setup to record membrane currents as soon as possible following the delivery of a NEP. Using this setup we obtained results consistent with the hypothesis originally proposed, namely that NEPs cause membrane depolarization by a novel mechanism, influx of Na+ through membrane 'electropores' or 'nanopores'. This in turn causes activation of voltage-gated Ca2+ channels and a rise in [Ca2+]i that is of sufficient magnitude to evoke Ca2+-dependent neurosecretion. We also unexpectedly found that Transient Receptor Potential or TRP channels serve as another pathway of Na+ entry into chromaffin cells exposed to NEPs, indicating that these channels are an important membrane target of NEPs that can affect cell excitability. Other novel effects of NEPs on chromaffin cell excitability that were revealed include differential electric field (E-field) and pulse-number effects on voltage-gated Na+ and K+ currents. The overall significance of these findings is that modulation of chromaffin cell excitability by NEPs occurs by two mechanisms, one involving the plasma membrane lipid bilayer (electropermeabilization) in concert with TRP channel activation that leads to Na+ influx, and one involving modulation of ion channel prot

15. SUBJECT TERMS
patch clamp electrophysiology, nanoelectropulses

Standard Form 298 (Rev. 8/98)
Prescribed by ANSI Std. Z39.18

16. SECURITY CLASSIFICATION OF:			17. LIMITATION OF ABSTRACT	18. NUMBER OF PAGES	19a. NAME OF RESPONSIBLE PERSON
a. REPORT	b. ABSTRACT	c. THIS PAGE			BRADSHAW, PATRICK
Unclassified	Unclassified	Unclassified	UU		19b. TELEPHONE NUMBER *(Include area code)* 703-588-8492

FINAL REPORT

FA9550-14-1-0018

Submitted to the AFOSR
Attention: Dr. Patrick Bradshaw

Nanoelectropulse-induced changes in cell excitability: a new approach for neuromodulation

Gale Louise Craviso, Ph.D.

University of Nevada, Reno School of Medicine
Department of Pharmacology
1664 N. Virginia Street/MS 318
Reno, NV 89557

TABLE OF CONTENTS

LIST OF FIGURES

1.0 SUMMARY

This multidisciplinary project has been to explore the potential for nanosecond-duration electric pulses (NEPs) to serve as a safe and potentially non-invasive approach for altering neural cell excitability, with the overall objective of developing new ways to enhance human performance. Our strategy combined experimental and computational approaches to elucidate how very short duration (less than 10 ns in duration) electric pulses of high intensity (>1 megavolt-per-meter; MV/m) alter the excitability of isolated bovine adrenal chromaffin cells, a leading non-transformed model of neurosecretion. Crucial to the success of the project was designing and fabricating a setup to record membrane currents as soon as possible following the delivery of a NEP. Using this setup we obtained results consistent with the hypothesis originally proposed, namely that NEPs cause membrane depolarization by a novel mechanism, influx of Na^+ through membrane "electropores" or "nanopores". This in turn causes activation of voltage-gated Ca^{2+} channels and a rise in $[Ca^{2+}]_i$ that is of sufficient magnitude to evoke Ca^{2+}-dependent neurosecretion. We also unexpectedly found that Transient Receptor Potential or TRP channels serve as another pathway of Na^+ entry into chromaffin cells exposed to NEPs, indicating that these channels are an important membrane target of NEPs that can affect cell excitability. Other novel effects of NEPs on chromaffin cell excitability that were revealed include differential electric field (E-field) and pulse-number effects on voltage-gated Na^+ and K^+ currents. The overall significance of these findings is that modulation of chromaffin cell excitability by NEPs occurs by two mechanisms, one involving the plasma membrane lipid bilayer (electropermeabilization) in concert with TRP channel activation that leads to Na^+ influx, and one involving modulation of ion channel proteins that are voltage-gated. Other accomplishments include the construction of an advanced 3D chromaffin cell model to show how the electric field affects, and in turn is affected by, intracellular organelles; initiating investigations into the efficacy of 5 ns versus the physiological stimulus for evoking Ca^{2+}-dependent exocytosis; and formalizing a collaboration with researchers at the AFRL in Fort Sam Houston, TX, to work toward practical applications of NEPs, in particular, a soldier worn "wearable" antenna system to increase warfighter performance via the "fight or flight response". As an overall accomplishment, the interdisciplinary nature of the project has provided invaluable basic research training opportunities for undergraduate, graduate, and post-graduate students in the basic sciences and in engineering.

2.0 INTRODUCTION

Nanosecond duration pulsed electric fields (NEPs) may well be a new modality for neuromodulation that provides short duration (low damage risk) and highly precise targeting of specific cells/tissues. In this AFOSR project we have been exploring this possibility using neuroendocrine chromaffin cells isolated from bovine adrenal glands as our cell model. Chromaffin cells are derived from the neural crest and share many similarities to sympathetic neurons, such as the synthesis, storage and release of catecholamines, which occurs by Ca^{2+}-dependent exocytosis, the same mechanism used by neurons to release neurotransmitters. As such, chromaffin cells are a leading, non-transformed model of neurosecretory/neural-type cells. Their simple, spherical cell morphology relative to the more complex morphology of neurons has been essential for this project since it has allowed the construction of cell models to help elucidate fundamental mechanisms based on the experimental results. In this way, we have been

able to derive a basic understanding of how NEPs modulate neural cell excitability, which will be important to guide future *in vivo* investigations aimed directly at using these ultrashort nanosecond electric pulses for practical applications relevant to the DoD.

As described in the RESULTS AND DISCUSSION section, we made significant progress identifying the mechanism of NEP-induced VGCC activation, one of the aims of the project. Significant progress was also made regarding how NEPs affect voltage-gated channels, also one of the aims of the project. Other accomplishments include 1) establishing the basis for why 5 ns pulses do not cause electroporating effects on membranes of intracellular organelles, a hallmark of NEPs; 2) construction of an advanced 3D cell model to understand how the presence of intracellular organelles affect other intracellular organelles in a cell exposed to an electric field, and 3) initiation of studies comparing the effectiveness of 5 ns pulses for evoking Ca^{2+}-dependent exocytosis relative to that evoked by the physiological stimulus, nicotinic receptor activation.

Finally, during the last year of funding we formalized a collaboration with Dr. Bennett Ibey and his research team at the AFRL in fort Sam Houston, TX, who are interested in targeted activation of the adrenal gland *in vivo* by developing a soldier worn "wearable" antenna system. The objective is to increase warfighter performance, via the "fight or flight response", in times of extreme need. Progress that has been made toward this collaborative effort is described.

3. METHODS

3.1 Isolation and culture of bovine adrenal chromaffin cells

Bovine chromaffin cells were isolated from the medulla of fresh adrenal glands obtained from Wolf Pack Meats, a USDA approved abattoir facility operated by the University of Nevada, Reno. Briefly, the outer cortex of the gland was removed by dissection and a catheter inserted into the adreno-lumbar vein of the medulla through which collagenase B was perfused to digest the tissue. Once digestion was complete, the swollen tissue was gently agitated to obtain single cells, which were subjected to four centrifugation steps. After the final centrifugation step, the cells were suspended in Ham's F-12 medium supplemented with 10% bovine calf serum, 100 U/ml penicillin, 100 μg/ml streptomycin, 0.25 μg/ml fungizone, and 6 μg/ml cytosine arabinoside, placed into tissue culture flasks and incubated for 5.5 hours at 36.5°C under a humidified atmosphere of 5% CO_2. Then, the chromaffin cells, which remain in suspension, were collected from each flask, pooled, distributed into Petri dishes, and maintained in suspension culture at 36.5°C under a humidified atmosphere of 5% CO_2 (1). For experiments, the large aggregates of cells that form in culture were dissociated into single isolated cells with the protease dispase (2). Once cell aggregates were fully dissociated, the cells were plated onto fibronectin-coated 35 mm glass bottom dishes or glass coverslips.

3.2 Fluorescence imaging

3.2.1 Intracellular Ca^{2+} level ($[Ca^{2+}]_i$)

Attached cells were incubated with the cell permeant Ca^{2+}-sensitive fluorescent indicator Calcium Green-1-AM (1 μM; 480/535 nm) for 45 min at 37°C in a balanced salt solution (BSS) with the following composition: 145 mM NaCl, 5 mM KCl, 1.2 mM NaH_2PO_4, 2 mM $CaCl_2$, 1.3 mM $MgCl_2$, 10 mM glucose, 15 mM HEPES and 0.1% bovine serum albumin, pH 7.4. After incubation, the cells were washed twice with BSS lacking bovine serum albumin and placed on

the stage of a Nikon TE2000 epifluorescence microscope equipped with a 100X objective. Bright field and fluorescence images of the cells were captured by an iXonEM + DU-897 EMCCD camera using the open source microscopy software Micro-Manager. Continuous baseline Ca^{2+} fluorescence of the cells was monitored 10 s prior to electric pulse application and continued for 50 s after the stimulus. Sequences were analyzed using the public-domain image processing program ImageJ. The change in fluorescence intensity (ΔF) of the cells was calculated by subtracting the background fluorescence from the fluorescence of the cell ($\Delta F = F_{cell} - F_{background}$). ΔF was then normalized to the fluorescence intensity value (F_0) at the time when the stimulus was applied ($\Delta F/F_0$). Bright field images of the cells were obtained before and after (typically 50 s) pulse exposure (3-5).

In some experiments, cells were stimulated with the mixed nicotinic-muscarinic cholinergic receptor agonist carbachol, or the selective nicotinic receptor agonist, 1, 1-dimethyl-4-phenyl-piperazinum (DMPP). The agonists were applied either to a single cell using a pressure ejection system, duration of application 5 ms (6), or to an entire dish of cells via perfusion (7).

3.2.2 Mitochondrial membrane potential

Cell medium was removed from a dish of attached cells and the cells washed twice with BSS. The cells were incubated with tetramethylrhodamine (TMRE, Ex/Em: 543/593 nm) at a concentration of 20 nM for 20 minutes at 36.5 °C in BSS. Then, the dye solution was removed and replaced with BSS, and the cells imaged as described for cells loaded with Calcium Green-1.

3.2.3 Exocytosis of fluorescently-labeled secretory granules.

Cell medium was removed from a dish of attached cells and the cells washed twice with BSS. The cells were incubated with acridine orange (3 μM, Ex/Em: 480/590-660 nm) for 15 minutes at room temperature. The dye solution was removed, replaced with BSS, and the cells incubated for 45 minutes at room temperature before total internal reflection fluorescence (TIRF) imaging using a Nikon 100X, 1.49 NA Apo TIRF objective, with the cells illuminated by an Argon Ion 488 λ laser.

3.3 Patch clamp electrophysiology

A coverslip containing attached cells was placed in a cell perfusion chamber positioned on the stage of an inverted Nikon TS-100 epifluorescence microscope. Cells were continuously perfused at a rate of 0.5 ml/min with BSS (same as above but lacking bovine serum albumin). The whole-cell variant of the patch clamp technique was used in voltage clamp mode to monitor NEP-evoked changes in membrane conductance (8). Briefly, a glass micropipette (tip diameter: 1 μm) was filled with an internal solution consisting of 10 mM NaCl, 30 mM KCl, 110 mM K-gluconate, 1 mM $MgCl_2$, 10 mM EGTA, 3 mM MgATP, and 10 mM Hepes, pH 7.2, and applied to a cell membrane using a motorized micromanipulator. After rupturing the plasma membrane to achieve the whole-cell recording mode, recordings were obtained at a holding potential of -70 mV with an Axopatch 200B amplifier and Digidata 1322A data acquisition system, and pClamp software at a sampling rate of 20 kHz and filtering at 2 kHz (8).

3.4 Cell exposure to 5 ns electric pulses

For the fluorescence imaging experiments, single or multiple 5-6 ns pulses were delivered to a chromaffin cell via a pair of electrodes consisting of two cylindrical gold-plated tungsten rods (127 μm diameter) spaced 100 μm apart. The tips of the electrodes were immersed in the BSS bathing the cells and placed 40 μm above the bottom of the dish (or coverslip) using a motorized

micromanipulator, with the target cell located at the center of the gap between the electrode tips. Single pulses with amplitudes that produced E-fields ranging from 2 to 21 MV/m at the location of the cell were generated by a custom-fabricated nanosecond pulse generator from Transient Plasma Systems (Torrance, CA). Depending on the pulse amplitude, the pulse width varied from 5 to 6 ns. As described in (6,7), the E-field distribution in the vicinity and at the location of the target cell was computed using the commercially available Finite-Difference Time-Domain (FDTD) software package SEMCAD X (version 14.8.5, SPEAG, Zurich, Switzerland).

For the patch clamp experiments, a patched chromaffin cell was exposed to a single or pair of 5 ns pulses using the same 5 ns pulse delivery setup as for fluorescence imaging. Before experiments got underway, we designed and fabricated a setup that would enable us to monitor changes in membrane conductance as soon as possible after a cell was exposed to a pulse. With the successful design and completion of this setup, membrane conductance measurements could be made after a delay of only 8 ms from the time a pulse(s) was delivered to a cell, as described in detail in (8). The setup also allowed for two sham exposures preceding the pulse or pulse-pair.

3.5 Numerical cell modeling

A 2D numerical cell model was constructed in MATLAB (2015a, Mathworks) for determining the E-field thresholds for plasma membrane and intracellular membrane electroporation of chromaffin cells exposed to 5 ns pulses. Computations were based on the meshed transport network method (MTNM) developed by Smith and Weaver (9) and the electrical response of the cell was based on the asymptotic model of electroporation developed by Neu and Krassowska (10). The cell parameters used to construct the cell model were, where possible, specific to chromaffin cells. Chromaffin cell plasma membrane properties were obtained from a patch-clamped cell. Cell membrane conductivity (σ_m) and permittivity (ε_m) were calculated from membrane resistance (R_m) and capacitance (C_m) values, respectively. Other properties such as cytoplasmic conductivity (σ_{cyto}) were derived by microfluidic impedance spectroscopy in combination with a constant phase element, Cole-Cole, Maxwell-Wagner mixture models and a granular cell model (11). All other electrical parameters were taken from the literature. Complete details are given in (6).

Briefly, the system geometry consisted of a circle of radius r_{cell} = 8 μm, centered inside a bounding box (system boundary) of dimensions 100 μm x 100 μm that represented the 100 μm gap between the electrodes. Four circular structures representing a nucleus, a mitochondrion, an endoplasmic reticulum (*ER*) and a secretory granule were placed arbitrarily offset from the cell center and had radii of r_{nucl} = 2.5 μm, r_{mito} = 1 μm (12), r_{ER} = 500 nm (threefold larger than the average radius of a secretory granule) and r_{gran} = 400 nm, respectively. The cell, endoplasmic reticulum and secretory granule were each assigned a single membrane that had a thickness of d_m = 5 nm; the nucleus and the mitochondrion were assigned double membranes structures. The averaged voltage trace of the actual pulses captured during experiments was used in the model.

A localized model geometry was also constructed that consisted of a circular structure of radius r_{ER} = 300 nm representing the endoplasmic reticulum and a cluster of thirteen secretory granules, each having a radius r_{gran} = 140 nm. The dielectric properties of the secretory granules (granule interior conductivity and granule membrane permittivity) were obtained by microfluidic impedance spectroscopy as described in (11).

A 3D cell model was next created in Sim4life (Speag, Zurich, Switzerland), using its Low Frequency (LF) solver with some novel features based on the Finite Element method. Complete details appear in a M.S. thesis.

4.0 RESULTS AND DISCUSSION

4.1 The mechanism underlying VGCC activation evoked by a 5 ns pulse in chromaffin cells is consistent with Na^+ influx via plasma membrane nanopores.

Significant progress was made characterizing the effects of 5 ns pulses on the plasma membrane and linking these effects to VGCC activation. As shown in Figure 1, a single pulse evokes an inward current (usually < 200 pA) that is carried primarily by Na^+ since replacement of extracellular Na^+ with the much less permeable N-methyl-D-glucamine ion ($NMDG^+$) reduces inward current amplitude by ~ 60 %. The probability that VGCCs contribute to the observed membrane response is minimized because VGCCs are known to activate at potentials ~ -20 to -30 mV and in all experiments, the holding membrane potential was set to -70 mV. These results support our hypothesis of Na^+ influx as the underlying mechanism of VGCC activation (4).

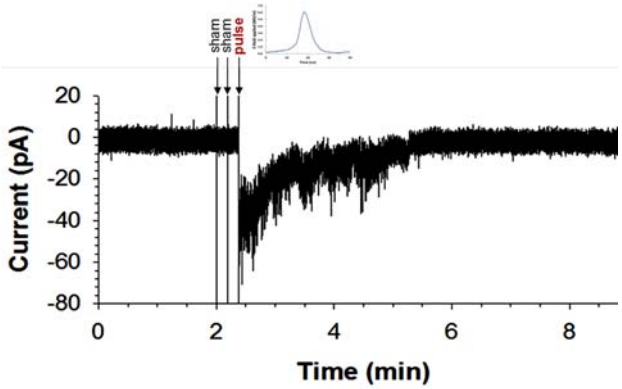

Figure 1. **NEP-evoked plasma membrane inward current recorded 8 ms after a 5 ns pulse was applied to a patched cell.** For the exposure, the cell was at a holding potential -70 mV. Current amplitude was greatest within the first 20 s and decayed exponentially toward baseline (0 pA) over the course of several minutes. (From ref. 8).

Additional experimental evidence in support of this conclusion are the following. Namely, the E-field threshold for evoking the inward current is similar to the threshold E-field for evoking Ca^{2+} influx via VGCCs. In this regard, if VGCC activation is due to plasma membrane permeabilization to Na^+, the E-field threshold for evoking each response should be similar since once the activation threshold of VGCCs is reached, VGCC activation will be all-or-none. As shown in Figure 2, this is the case. The threshold for each response, defined as the lowest field magnitude where a response is observed, is approximately 3 MV/m. Thus, we have directly linked plasma membrane permeabilization to a physiological response, Ca^{2+} influx into the cell through VGCCs.

Cell modeling also played an important role in linking NEP-induced changes in plasma membrane conductance with plasma membrane nanopore formation. As described in METHODS, we constructed a 2D cell model to simulate the electroporation of the plasma membrane by a 5 ns pulse. At the time the simulations were initiated, the cytoplasmic conductivity (σ_{cyto}) and other dielectric properties of bovine chromaffin cells were unknown. We collaborated with Michael Stacey (Frank Reidy Research Center for Bioelectrics) and his colleague Ahmet Can Sabuncu (now at Worcester Polytechnic Institute) to derive estimates of some of the dielectric properties of these cells rather than relying on values in the literature that were based on other cell types and therefore may not apply. For the determinations we used

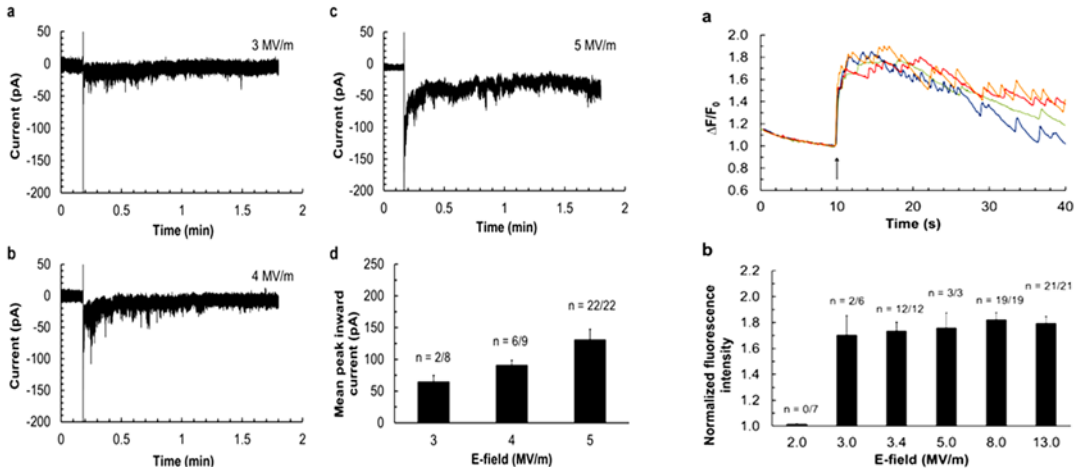

Figure 2. E-field threshold for plasma membrane permeabilization and Ca^{2+} influx via VGCCs. Left: Representative inward current responses obtained from whole-cell recordings of membrane conductance following exposure of patch-clamped cells to a 5 ns pulse applied at E-field amplitudes of 3 MV/m (a), 4 MV/m (b) and 5 MV/m (c). The vertical line indicates the time at which the pulse was applied. Shown in (d) is the mean peak inward current of the cells ± range for 3 MV/m, and ± s.e for 4 and 5 MV/m; $p > 0.05$. Right: Representative Ca^{2+} responses obtained by fluorescence imaging of $[Ca^{2+}]_i$ in chromaffin cells exposed to a 5 ns pulse applied (arrow) at an E-field amplitude of 3.4 MV/m (a). Shown in (b) are the mean of the peak responses of the cells ± s.e. In both bar graphs, n represents the number of cells responding to the pulse out of the total number of cells tested at each E-field amplitude (From ref. 6).

impedance spectroscopy in a granular cell model, which took into account the presence of the multitude of catcholamine-storing secretory granules in the cytoplasm (11). As shown in Figure 3, the numerical simulations show an E-field threshold of just under 3 MV/m for plasma membrane electroporation when using the derived value of σ_{cyto} =0.49 S/m. Thus, the numerically computed E-field threshold for membrane electroporation obtained from 2D cell modeling is similar to the experimentally-determined value. Achieving such agreement ensures that our cell model validates the mechanism responsible for the experimental results.

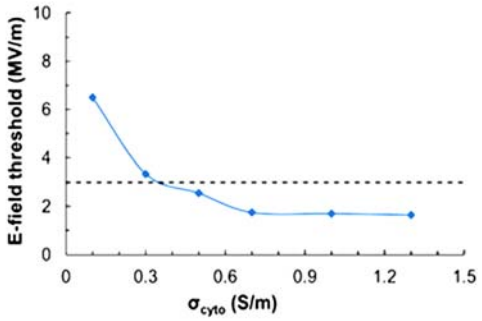

Figure 3. E-field threshold required for plasma membrane electroporation computed in the 2D cell model. Plasma membrane electroporation in the cell model is plotted as a function of cytoplasmic conductivity and E-fields ranging from 1 to 20 MV/m. The black dashed horizontal line on the plot indicates the 3 MV/m E-field threshold for permeabilization found experimentally (From ref. 6).

4.1.1 Significance

The finding that NEPs generate ion-conducting lipid nanopores that alter neural cell activity is novel, thereby broadening existing concepts of ways to modulate cell excitability through the use of ultra-short, high intensity electric pulses. Thus, Na^+ influx via plasma membrane nanopores

(electropores) could serve as an alternative depolarizing mechanism typically performed by activation of cation-permeable nicotinic cholinergic receptors, which is the mechanism for VGCC activation in chromaffin cells *in vivo*. This point takes on added significance since the lipid bilayer itself assumes a new role in response to a NEP, that of an electric field-induced modulator of membrane conductivity that replaces a function typically ascribed to protein ion channels, membrane depolarization.

4.2 Plasma membrane electronanoporation does not cause irreversible damage to the basal electrical properties of chromaffin cells exposed to a 5 ns pulse.

Overall our strategy has been to investigate first the effects of a single 5 ns, 5 MV/m pulse on chromaffin cell excitability, then extend our investigations to include effects evoked by multiple pulses. Such an investigation is important because effective neuromodulation will rely on establishing "patterns" of NEP delivery that elicit a desired outcome without causing adverse effects.

We have found that a second pulse delivered 5 s after the first pulse can evoke another rise in $[Ca^{2+}]_i$ that can result in an equivalent amount of released catecholamine (unpublished). Given that electronanoporation underlies VGCC activation, we therefore investigated the effect of two consecutive 5 ns pulses directly on plasma membrane conductance. As shown in Figure 4, a second pulse delivered 10 min after the first pulse elicited a similar response. Shortening the interpulse interval enhanced the magnitude of the NEP-induced inward current (Figure 5), suggesting a short refractory period. In fact, the recovery of this process followed a bi-exponential time course with time constants ≈ 200 ms and ≈ 20 s, respectively.

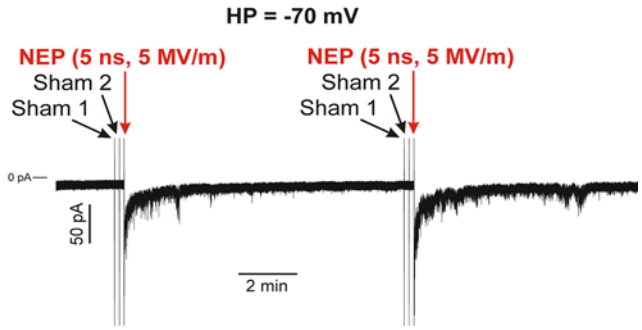

Figure 4. Effect of two 5 ns pulses with a long interpulse delay on plasma membrane inward current. The second pulse was delivered 10 minutes after the first pulse.

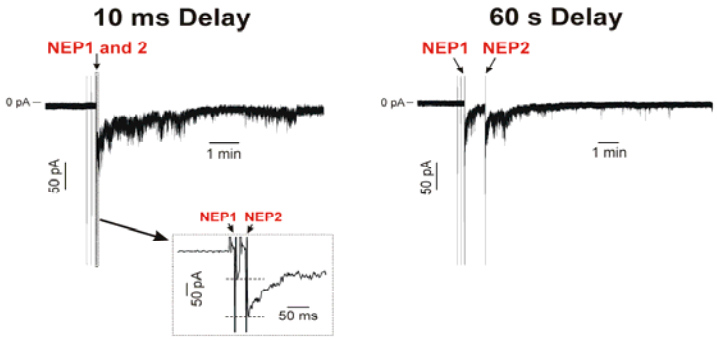

Figure 5. Effect of two 5 ns pulses with a short interpulse delay on plasma membrane inward current. The second pulse was delivered either 10 ms (left) or 60 s (right) after the first pulse. The inset on the bottom left is a blown-up view of the inward current for each pulse.

4.2.1 Significance

These results showing that a second 5 ns pulse has a secondary effect on inward current explains the ability of a second pulse to again trigger VGCC activation. Thus, NEPs do not inflict irreversible damage to the basal electrical properties of adrenal chromaffin cells and demonstrate the feasibility of applying multiple NEPs to control their excitability.

4.3 The biophysical properties of the plasma membrane conductance elicited by a single 5 ns pulse in chromaffin cells suggest that the NEP-induced membrane current is carried, at least in part, by a transmembrane voltage-independent ion channel.

As described above, we attributed the basal membrane current elicited by a single 5 ns pulse to hypothetical nanopores (so-called "electropores", "electronanopores") forming a hydrophilic pathway permitting ions to flow down their respective electrochemical gradient. However, although we and other researchers in the field typically use the term "pore", a lot more work needs to be carried out to fully understand the biophysical nature of the membrane conductance evoked by NEPs. For example, computer simulations using Molecular Dynamics at atomic level resolution that were conducted by our co-investigator Dr. Tom Vernier at ODU (AFOSR FA9550-14-1-0023) revealed that a single NEP can create and stabilize a hydrophilic pore tunnel formed by bridged phospholipid heads lowering the energy barrier for water and ion transport across the membrane. Interestingly, these electronanopores were shown to generally last less than 100 ns, indicating that they cannot account for the fact that the membrane conductance triggered by a single 5 ns pulse can last several tens of seconds to minutes following a pulse (see Figure 1). In this regard too, Pakhomov and Pakhomova (13) reported that so-called "nanopores" have properties consistent with those of ion channels, one being inward rectification. We have similarly found that a 5 ns pulse induces an inwardly rectifying current at a holding potential of -70 mv (Figure 6), displaying a reversal potential that is consistent with a non-selective cation conductance.

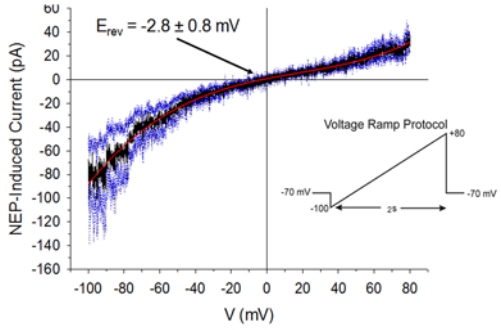

Figure 6. Inward rectification of the plasma membrane current evoked by a 5 ns pulse. The current traces were obtained using the voltage ramp protocol depicted by the schematic at the lower right. The red line is the average of the current (n = 5).

While investigating this finding during the last year of funding, we quite unexpectedly found that a large component of the membrane conductance pathway activated by a 5 ns pulse displays properties that are consistent with those of Transient Receptor Potential or TRP channel. These channels are a well-characterized but very diverse superfamily of cation-selective ion channels that are known to be regulated by a wide variety of stimuli including natural and synthetic chemical agents, pH, membrane stretch, temperature, and many others. As shown in Figure 7,

non-specific blockers of TRP channels inhibited the NEP-induced plasma membrane conductance by ~ 40-60%.

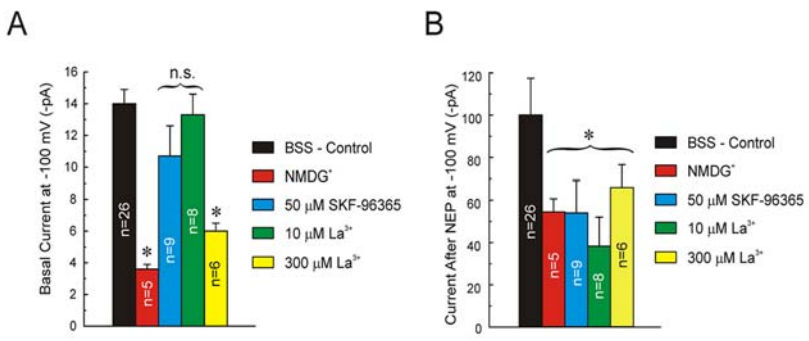

Figure 7. Pharmacological properties of basal and NEP-induced membrane currents. (A) Bar graph showing the effects of various conditions on mean basal membrane current registered at a holding potential of -100 mV. (B) Bar graph showing the effects of the same conditions as in panel A immediately after the application of a 5 ns pulse. For both panels, each bar is the mean ± s.e.m. with the number of cells indicated within each bar. *: significantly different from BSS – Control. n.s.: not significant.

As to the mechanism involved, we next addressed the possibility that NEPs altered membrane phospholipids in a way that leads to activation of TRP channels. For the analysis, several agents were employed either alone or in combination. These included wortmannin, an inhibitor of PIP_2 synthesis, methyl-β-cyclodextrin (MβCD) that depletes plasma membrane cholesterol, and TRP channel blockers. As shown in Figure 8, wortmannin and MβCD had no effect on the basal membrane current recorded at a holding potential of -100 mV whereas there was significant inhibition of the NEP-induced current.

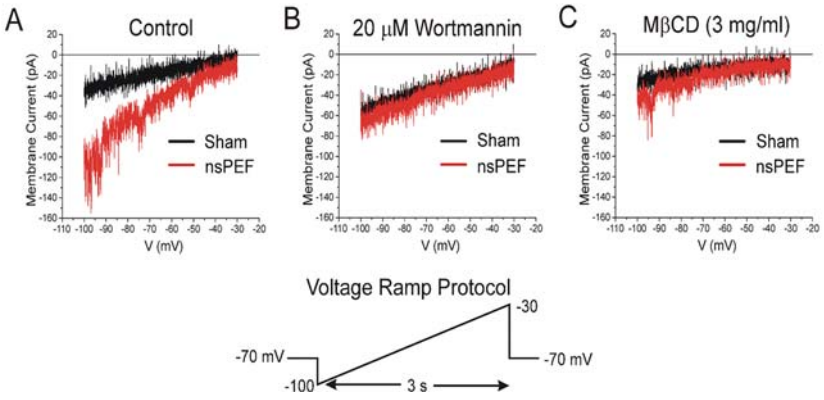

Figure 8. Effect of inhibiting PIP_2 synthesis or depleting membrane cholesterol on the NEP-induced inward current. The current traces were obtained using the voltage ramp protocol depicted by the schematic at the bottom.

Figure 9 shows further that inhibition of PIP_2 synthesis, depletion of membrane cholesterol or blocking TRP channels produced the same amount of inhibition on the NEP-induced membrane conductance. Figure 9 also importantly shows that there were no additive effects when all three agents were combined. These results strongly suggest that the three agents targeted different levels of the same pathway resulting in the full effect.

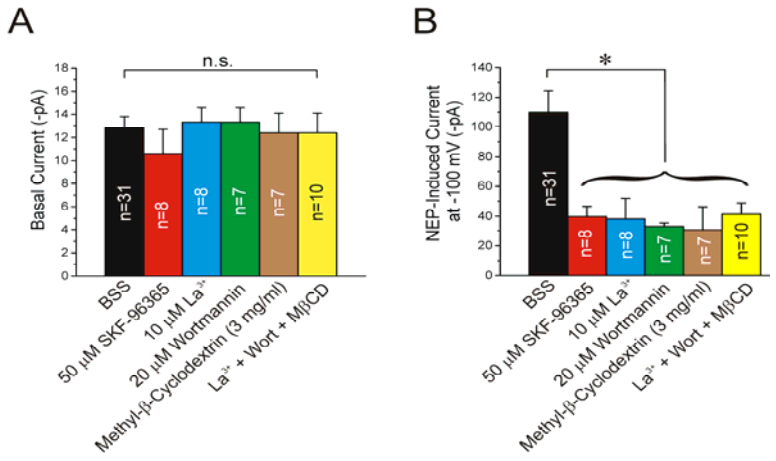

Figure 9. Effect of inhibiting PIP_2 synthesis, membrane cholesterol depletion or blocking TRP channels on the NEP-induced membrane conductance. (A) Bar graph showing the effects of various pharmacological agents on mean basal membrane current recorded at the HP of -100 mV. (B) Bar graph showing the effects of the same conditions as in panel A immediately after the application of the NEP. *: significantly different from BSS – Control. n.s.: not significant.

4.3.1 Significance

Our data support the idea that a significant fraction of the current evoked by NEPs may be carried by Na^+-permeable TRP channels. Although it is possible that membrane cholesterol depletion altered the biophysical properties of the membrane in a way that could prevent or limit the formation of lipid-containing electronanopores, an equally attractive and perhaps more plausible hypothesis is that lipid rafts (and caveolar disruption?) altered TRP trafficking and/or compartmentalization leading to a diminished ability of NEPs to activate these channels. Another possibility that is not mutually exclusive is that NEPs may cause depletion of PIP_2, which may play a permissive role for TRP channel activity. A manuscript describing these very recent findings and their implications is near completion.

4.4 A single 5 ns pulse produces differential E-field-dependent inhibitory effects on voltage-gated ion channels in chromaffin cells.

In addition to the ability of a 5 ns pulse to alter chromaffin cell excitability by allowing Na^+ to cross the plasma membrane via nanopores/and or channels and depolarize the membrane, overall cell excitability could be further affected if the pulse also exerted effects on voltage-gated ion channels. One of our proposed specific aims was to investigate this possibility. To this end, we carried out whole-cell patch clamp experiments in chromaffin cells to determine the effect of a single 5 ns pulse on macroscopic ion currents, which in these cells comprise a mixture of Na^+, Ca^{2+} and K^+ currents. Our experimental approach utilized conditions designed to simulate near physiological ion gradients and the whole-cell recording system developed during the first year of funding to study effects with a very short delay after pulse delivery (8).

We first determined the general biophysical properties of peak inward and outward currents during voltage steps and membrane current stability over time following membrane rupture. Consistent with what is found in older literature in this cell type (14,15), the early peak inward current is primarily composed of a fast voltage-dependent Na^+ current (I_{Na}), whereas the late outward current is composed of at least three ionic currents: a voltage-gated Ca^{2+} current (I_{Ca}), a

Ca^{2+}-activated K^+ current ($I_{K(Ca)}$), and a sustained voltage-dependent delayed rectifier K^+ current (I_{KV}).

Because of the unique capabilities of our patch-clamp/NEP exposure setup, we could first record the membrane permeabilizing effect of the pulse (represented by I_{leak}) and start probing effects on voltage-gated ionic currents in the same cell by applying a voltage step to +10 mV from a holding potential of -70 mV. Our primary findings, which are reported in (16), are as follows. Inward current (Figure 10, left): a single pulse applied at an E-field amplitude of 5 MV/m resulted in an instantaneous decrease of ~4% in peak I_{Na} that then declined exponentially to a level that was ~85% of the initial level after 10 min. Increasing the E-field amplitude to 8 or 10 MV/m caused a twofold greater inhibitory effect on peak I_{Na}. The decrease in I_{Na} was associated with a decrease in maximal Na^+ conductance. Outward current (Figure 10, right): for cells exposed to a pulse at 5 MV/m there was no effect on late outward current. When the E-field was increased to 8 or 10 MV/m, late outward current in some cells (3 out of 10 cells and 6 out of 11 cells for 8 and 10 MV/m, respectively) underwent a progressive ~20 to 25% decline over the course of the first 20 s following pulse exposure.

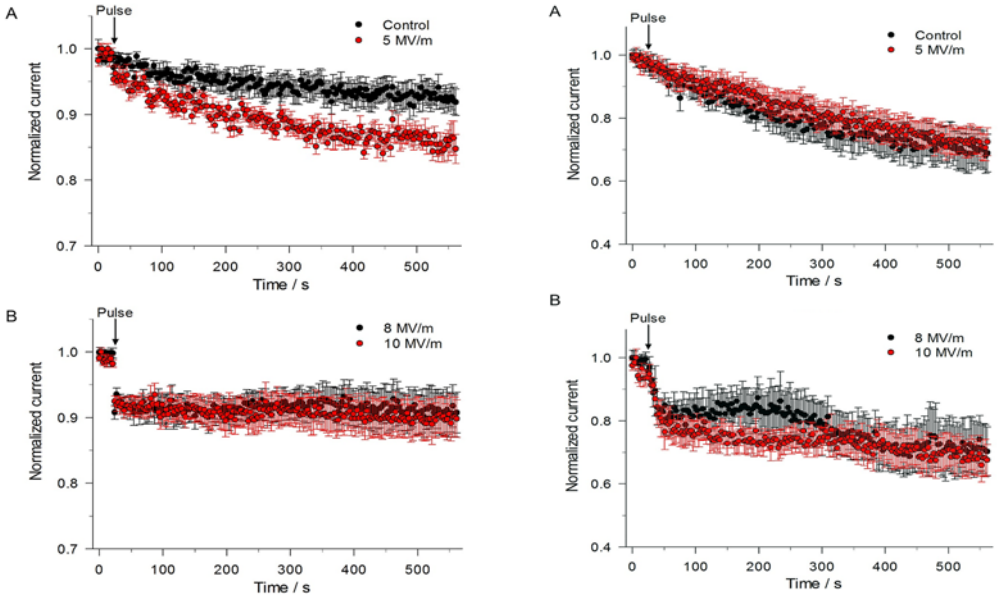

Figure 10. Early inward and late outward current response to a single 5 ns pulse as a function of E-field amplitude. Left: Time course of the changes in peak inward current for an unexposed cell (control) compared to a cell exposed to a 5 ns, 5 MV/m pulse (A), and for a cell exposed to a 5 ns pulse at E-fields of 8 MV/m and 10 MV/m (B). Right: Time course of the changes in mean outward current for the same cells shown at the left for peak inward current. Data are expressed as the mean ± s.e. (From ref. 16).

4.4.1 Significance

These results demonstrate that a 5 ns pulse affects plasma membrane ion channels important for cell excitability, and that the E-field amplitude of the pulse determines not only the magnitude of the effect but also which ion channels are impacted. The significance of this finding is that modulation of chromaffin cell excitability by NEPs occurs by two mechanisms, one involving the lipid bilayer and one involving ion channel proteins. This in turn raises the possibility that the contribution of each can be manipulated as function of the particular pulsing scheme employed.

Questions our findings raise include the physiological significance of the effects on plasma membrane ion channels (i.e., the influence on cell excitability), the basis for the different sensitivity of the channels to the E-field amplitude, as well as the mechanism underlying the effects (i.e., does a pulse directly affect channel protein or indirectly through an alteration of the lipid environment surrounding the channel). In general, the inhibition of voltage-gated ion channels by NEPs, especially in light of possible differences in sensitivity to E-fields, has many potential implications. With respect to Na^+ channels, for example, selective targeting of these channels by NEPs could be used to block nerve conduction by mimicking the activity of local anesthetics.

4.5 Na^+ conductance via voltage-gated ion channels in adrenal chromaffin cells is differentially modulated by single vs twin 5 ns pulses.

As described above, we have been examining membrane responses of chromaffin cells evoked by two, consecutive 5 ns pulses (twin pulses or a pulse-pair). With respect to how a pulse pair affects $I_{Na,}$ we found something quite remarkable. The application of a second 5 ns pulse 30 s after the first pulse amplified the instantaneous inhibitory effect of a single pulse on I_{Na} from ~4% to 7% (Figure 11). The enhanced inhibitory effects of twin vs single pulses on I_{Na} were not due to a shift in the voltage-dependence of steady-state activation and inactivation but were associated with a reduction in maximal Na^+ conductance. Interestingly, and in contrast to the effects of a single pulse, the application of a second pulse led to a progressive recovery of the current that stabilized near the level of I_{Na} observed in control cells unexposed to NEPs. Increasing the time interval between the twin pulses from 30 to 60 s led to similar inhibition of (~ 7%) and recovery of I_{Na} (data not shown).

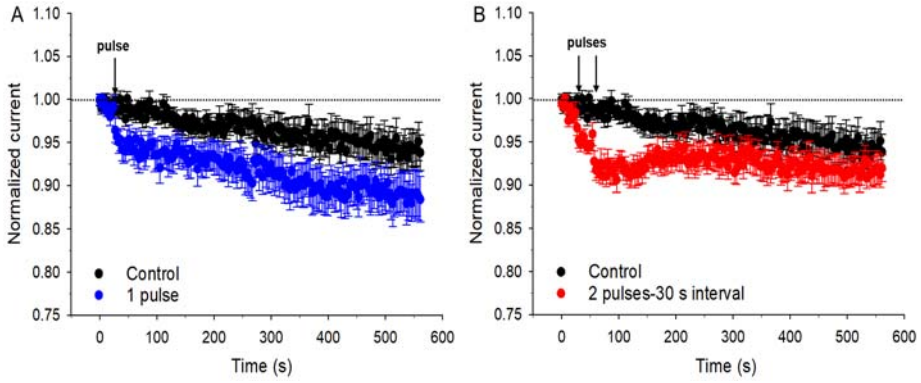

Figure 11. Effects on I_{Na} of a single or twin 5 ns pulses applied at an E-field of 5 MV/m. (A) Time course of changes in I_{Na} for unexposed cells (Control, black circles) compared to cells exposed to a single pulse (blue circles). (B) Time course of changes of I_{Na} in cells exposed to twin pulses applied with a 30 s gap (red circles) compared to that recorded in unexposed cells (Control, black circles). Each data point is a mean ± s.e (Control, n = 20; 1 pulse, n = 12; 2 pulses-30 s interval, n = 10).

As shown in Figure 12, we next found that decreasing the time interval between the twin pulses from 30 to 5 s again produced a similar inhibitory effect on I_{Na} (~ 7%). However, the recovery of I_{Na} was accelerated and enhanced relative to longer delays between pulses. Further shortening the time interval between the two pulses to 1 s (~ 6%), 100 ms (~ 5%) or 10 ms (~ 3%) progressively attenuated the inhibitory effect on I_{Na}. Again, shorter delays accelerated and amplified the recovery of I_{Na}. In fact, when the delay was only 10 ms, the shortest interval

achievable with our exposure setup, the current leveled off near that recorded at the beginning of the experiment, that is, prior to the application of NEPs.

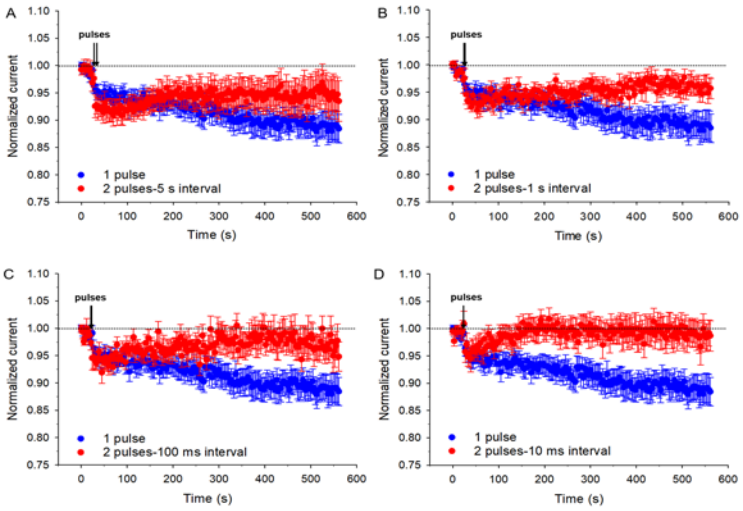

Figure 12. Effects on I_{Na} of the time interval between twin 5 ns pulses applied at an E-field of 5 MV/m. Time course of changes in I_{Na} for cells exposed to a single pulse (blue circles) compared to cells exposed to twin NEPs (red circles) separated by a 5 s (A), 1 s (B), 100 ms (C) or 10 ms time interval (D), respectively. Each data point is a mean ± SE (1 pulse, n = 12; 2 pulses with 5 s interval, n = 9; 2 pulses with 1 s interval, n = 9; 2 pulses with 100 ms interval, n = 9; 2 pulses with 10 ms interval, n = 9).

An additional major finding is that disruption of lipid rafts by depleting membrane cholesterol with methyl-β-cyclodextrin (MβCD) enhanced the inhibitory effects of twin NEPs on I_{Na} and ablated the progressive recovery of this current at short twin pulse intervals. These findings suggest that twin NEPs influenced membrane lipid rafts in a manner that enhanced the trafficking of newly synthesized and/or recycling of endocytosed voltage-gated Na^+ channels.

4.5.1 Significance

Our results showing that the effect of a 5 ns pulse on I_{Na} can be modulated in a unique manner by applying a pair of pulses point to additional ways in which NEPs could potentially be applied to fine tune cell excitability. That is, a pulse pair having a very short interpulse interval (10 ms) can not only attenuate the inhibitory effect of a pulse on I_{Na} but also reverse any run-down of the current over the course of a long stimulation period. Twin pulses having an interpulse interval also of 10 ms and applied at 5 MV/m, while having no inhibitory effect on late outward current, actually prevent rundown of the current over the course of a long stimulation period. While we do not yet understand the mechanisms involved, these results point to new considerations with respect to establishing "patterns" of NEP delivery that elicit a desired outcome without causing adverse effects. In other words, perhaps NEPs should be delivered as pulse-pairs. A manuscript describing these findings and their implications has been submitted for publication.

4.6 High E-field amplitudes (8 MV/m and higher) are required to porate the membranes of intracellular Ca^{2+} storing organelles in chromaffin cells.

A 5 ns, 5 MV/m pulse can excite chromaffin cells and cause Ca^{2+} influx that triggers exocytosis and catecholamine release without causing additional, unwanted effects on intracellular structures that store Ca^{2+}, such as membrane poration that would cause Ca^{2+} release into the

cytoplasm. Such an effect on the endoplasmic reticulum has been described in a variety of cell types exposed to NEPs.

Ca^{2+} imaging experiments determined that much higher E-fields are required to porate the membranes of intracellular Ca^{2+}-storing organelles (in chromaffin cells, these are the endoplasmic reticulum and catecholamine-storing secretory granules) than for triggering Ca^{2+} influx via VGCCs. These results are shown in Figure 13 where Ca^{2+} release is first detectable in some cells at an E-field amplitude of ~8 MV/m, which we call the "threshold". Also shown is that the number of cells responding to the pulse as well as the magnitude of the Ca^{2+} response increases as the E-field amplitude increases. Regardless, the magnitude of the changes in $[Ca^{2+}]_i$ that were observed were not very pronounced, demonstrating that a 5 ns pulse even at high E-field amplitudes is not very efficient at mobilizing Ca^{2+} from internal stores in these cells.

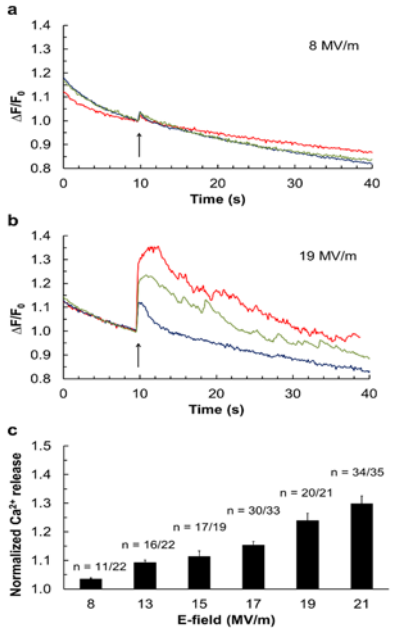

Figure 13. E-field threshold for evoking Ca^{2+} release from intracellular stores determined by fluorescence imaging in the absence of extracellular Ca^{2+}. The traces shown in (a) and (b) are typical responses observed in cells exposed to a single pulse (arrow) applied at E-field amplitudes of 8 and 19 MV/m, respectively. Shown in (c) is the magnitude of the Ca^{2+} response as a function of the applied E-field represented as the mean of the peak responses ± s.e.; $p < 0.05$. In each case, n represents the number of cells responding to the pulse out of the total number of cells tested at each E-field amplitude (From ref. 6).

Additional studies, details of which are reported in (7), verified that the Ca^{2+}-storing organelle from which NEP evokes Ca^{2+} release is the endoplasmic reticulum and not secretory granules. This was accomplished by demonstrating that under conditions in which the endoplasmic reticulum was fully depleted of Ca^{2+}, release of Ca^{2+} from internal stores in response to a pulse was never observed. Moreover, in simulations we had used the measured dielectric properties of the secretory granules (11) where it was found that secretory granule membranes electroporate at an E-field amplitude greater than 22 MV/m. Thus, secretory granules are likely not a target for poration in chromaffin cells exposed to E-field intensities lower than 22 MV/m. This finding is consistent with experiments demonstrating that the ER is the internal structure that is porated and hence the source of the Ca^{2+} that is released in response to pulses applied below 22 MV/m.

We also determined that Ca^{2+} is released from both IP_3- and caffeine-sensitive endoplasmic reticulum Ca^{2+} stores. Importantly, however, each store is differentially involved. Specifically, Ca^{2+} release due to membrane poration occurs primarily from caffeine-sensitive stores and is responsible for the instantaneous increase in Ca^{2+} shown in Figure 13. In contrast, Ca^{2+} spikes that are observed at the higher E-fields and at various times after the pulse (Figure 14) are associated with Ca^{2+} release mediated by IP_3 receptors. These results are the first to demonstrate that a single NEP can differentially affect endoplasmic reticulum Ca^{2+} stores, resulting in heterogeneous Ca^{2+} responses.

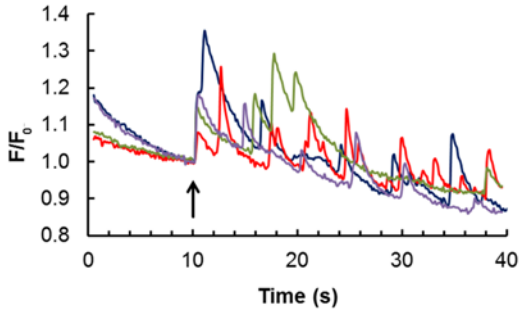

Figure 14. Ca^{2+} spikes in chromaffin cells exposed to a single 5 ns, 17 MV/m pulse in the absence of extracellular Ca^{2+}. Representative traces of Ca^{2+} spikes in chromaffin cells exposed to a single 5 ns pulse. The arrow indicates when the pulse was delivered to the cells (From ref. 7).

As reported in (6), we used 2D cell models to gain a better understanding of the mechanisms involved in the differential effects of NEPs on the membranes of intracellular organelles versus the plasma membrane in chromaffin cells. One of the possibilities we considered was that the large number of secretory granules present in the cytoplasm (> 10,000 per cell) and which occupy 20 - 30 % of the cell interior may play a role, such as having a shielding effect on the endoplasmic reticulum by attenuating the E-field inside the cell. Figure 15 shows the "localized" model that was used for the simulations wherein structures representing a cluster of

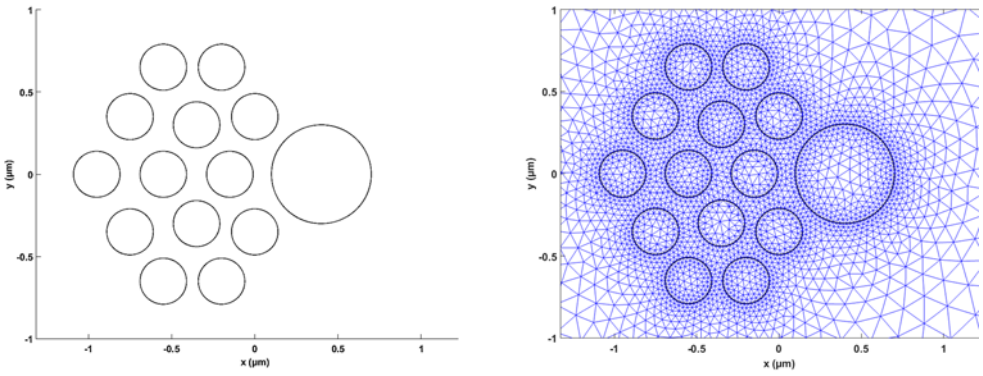

Figure 15. Localized model to assess shielding of the endoplasmic reticulum by secretory granules. The geometry of the localized model (left) consisted of a circular structure representing the endoplasmic reticulum. Thirteen circular structures representing discrete secretory granules were placed as a cluster near the endoplasmic reticulum. The corresponding mesh is shown at the right.

secretory granules were placed on one side of the endoplasmic reticulum. The simulations showed no apparent shielding effect by the secretory granules on the endoplasmic reticulum, leading us to conclude that a more realistic 3D model of a chromaffin cell may be what is needed. That is, including as many secretory granules in the cytoplasm as possible. To this end, a numerical chromaffin cell model to study the effects of secretory granules on the E-field and transmembrane potential (TMP) distribution of the granules, the nucleus and the cell membrane was created. The program in which this model was created was Sim4life, a software package based on the FDTDomain method using its Low Frequency (LF) solver with some novel features based on the Finite Element Method (FEM). A Beta-version of this LF FEM solver, which is in the final stages of development, has the ability to generate complex structures. Access to the Beta-version was given to one of our graduate students when he obtained a ThinkSwiss scholarship to spend two months at IT'IS Foundation in Zurich, which has a research alliance partnership with Speag.

Figure 16 shows one of the geometries investigated. It consists of a spherical chromaffin cell (radius of 8 μm), a nucleus of radius 2.5 μm located off-center (as in a real chromaffin cell), 500 granules of radius 0.2 μm located randomly within a distance of 2 μm from the nucleus, and 500 granules located randomly in the remaining cytosol. The geometry was meshed using the mesher in Sim4life into tetrahedral meshcells, and simulated using the LF solver in Sim4life alluded to above. The LF solver is a quasi-static solver that solves Maxwell's equations using the Finite Element method. It was not capable of taking a time-varying pulse as input and hence we have solved for the potential and E-field distributions in the chromaffin cell model at single frequencies. The single frequencies chosen spanned the Fourier transform spectrum of the nanosecond pulse used in the laboratory in experiments. It was determined that 90% of the energy was present in the frequency range DC to 10 MHz. Hence, E-field and potential distributions were obtained at chosen frequencies in this range; the TMP was computed from the potential distribution.

We found that granules located in the vicinity of the equatorial side of the nucleus (within the solid white circles in Figure 17) have a higher TMP than the rest of the granules. In contrast, the granules located in the vicinity of the poles of the nucleus (within the dotted white circlesin Figure 17) have a lower TMP. In addition, depending on the location of the granules relative to the nucleus, the TMP distribution pattern can be tilted. These results show for the first time that the presence of the nucleus has an influence on the TMP of surrounding organelles, in this case, secretory granules. They further indicate that the sphere of influence extends approximately 2 μm from the nuclear membrane.

When the modeling got underway, multiple attempts to incorporate a more realistic endoplasmic reticulum in the cell model were unsuccessful due to a limitation of Sim4life to handle the complex geometrical features of this organelle. However, additional capabilities that were later added to Sim4life have since enabled us to create a fairly complex model of the endoplasmic reticulum, the first such model of this organelle that has been achieved to date. In the model, the rough endoplasmic reticulum consists of spherical dense sheets that surround the nucleus, and the smooth endoplasmic reticulum consists of tubular bodies that are distributed within the cytosol. Another important feature of the model is that all membranes have a realistic thickness of 5 nm. We have generated many results with this refined geometry of the endoplasmic reticulum, an example of which is depicted Figure 18. What is shown is that the direction of the E-field determines where the maximum TMP occurs in a membrane, thereby creating different TMP patterns with different magnitudes that in turn can lead to different

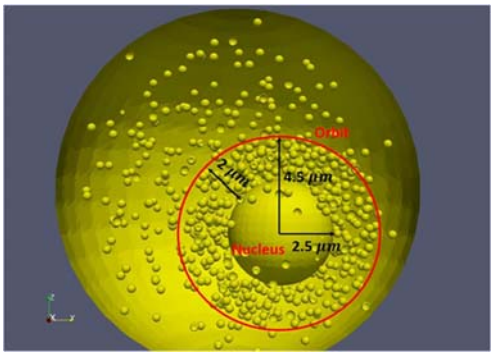

Figure 16. Schematic of the chromaffin cell geometry created in Sim4life for the 3D cell model.

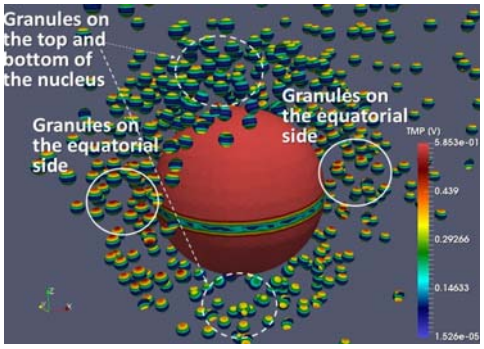

Figure 17. Zoomed-in view of the nucleus and secretory granules in the 3D cell model. The large red sphere represents the nucleus and the smaller spheres represent the granules. The TMP scale has been adjusted to better visualize the TMP of the granules.

poration schemes. Also, irregularities in the endoplasmic structure itself (such as folds) too can cause different TMP schemes and hence poration patterns. The simulations indeed could explain why release of Ca^{2+} from the endoplasmic reticulum sometimes appears to originate at discrete sites within a cell.

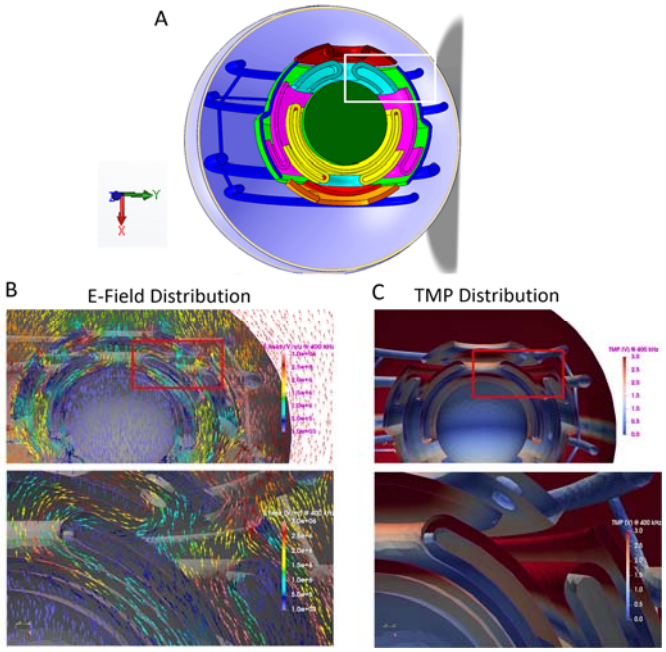

Figure 18. Analysis of the E-field and TMP in the inner sheets of the rough endoplasmic reticulum. (A) Geometry of the endoplasmic reticulum. (B) Arrow plot of the E-field distribution on the inner sheets of the rough endoplasmic reticulum (top). Zoomed-in view of the area outlined in red (bottom). (C) TMP distribution of the inner sheets of the rough endoplasmic reticulum (top). Zoomed-in view of the area outlined in red (bottom).

We are in the process of compiling the results for publication. Due to the volume and complexity of the results obtained for the analysis of the endoplasmic reticulum, they will

constitute a separate manuscript from that in which we are exploring how the presence of secretory granuels affects the TMP of the endoplasmic reticulum.

We point out that our ability to create such a model was the result of our student spending a few days during January 2018 at IT'IS Foundation in Switzerland learning how to use the new features of Sim4life.

4.6.1. Significance

Ca^{2+} mobilization from intracellular stores has served as an indicator of endoplasmic reticulum membrane poration in cells exposed to NEPs in the absence of extracellular Ca^{2+}. Determining that in chromaffin cells the porating effect of a 5 ns pulse applied at a near threshold E-field for cell stimulation appears to be confined to the plasma membrane is important since it indicates that adverse effects of NEP exposure on intracellular organelle membranes are unlikely. As described above, cell modeling has played an essential role in helping to explain these experimental results as well as to provide new insights into how the ultrastructural features of a cell influences its response to the intracellular effects of NEPs.

4.7 Ca^{2+} responses evoked by 5 ns pulses correlate with enhanced secretory efficacy in chromaffin cells.

In studying the effect of 5 ns pulse on chromaffin cells, our approach has included a comparison of NEP-evoked effects with those evoked by a nicotinic cholinergic receptor agonist. We found that the increase in $[Ca^{2+}]_i$ evoked by a single pulse significantly outlasts that evoked not only by a single application of the agonist but also five or even ten applications of the agonist (Figure 19). One possibility that could explain the longer recovery time for $[Ca^{2+}]_i$ to return to baseline levels in cells exposed to 5 ns pulses is that the penetration of the E-field into the cell disrupts mitochondrial membrane potential. This disruption would slow the rate of Ca^{2+} uptake into mitochondria, which is the main mechanism by which Ca^{2+} that enters a cell via VGCCs is rapidly removed from the cytoplasm to achieve baseline levels. To explore this possibility, mitochondria were labeled with the mitochondrial membrane potential dye

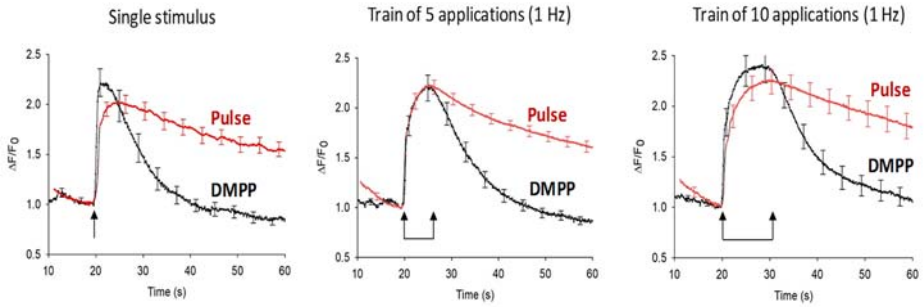

Figure 19. Comparison of the duration of Ca^{2+} responses in cells exposed to 5 ns pulses versus a nicotinic receptor agonist. Ca^{2+} responses were obtained by fluorescence imaging of $[Ca^{2+}]_i$ in cells exposed to one (left), five (middle) or ten (right) pulses or applications of 100 µm DMPP. Shown are averaged traces ± s.e. Arrows indicate when the stimulus or stimulus train was applied to the cells.

tetramethylrhodamine methyl ester (TMRE). If an applied stimulus disrupted mitochondrial membrane potential, the effect would be observed as a decrease in fluorescence at the time the pulse is delivered to the cell. We found that exposing cells to a single 5 ns pulse did not lead to a

decrease in TMRE fluorescence. Moreover, five and ten pulses applied at 10 Hz caused only minor (<2 %) transient decreases in TMRE fluorescence in some cells. From these results we concluded that the slower return of $[Ca^{2+}]_i$ to pre-stimulus levels relative to that for nicotinic cholinergic receptor stimulation does not involve disruption of mitochondrial membrane potential. Instead, given that the time course of the plasma membrane inward current evoked by a 5 ns pulse is on the order of minutes (see Figure 1), we are exploring the possibility that the plasma membrane remains depolarized to a level that is sufficient to permit VGCCs to remain open for an extended time.

Regarding physiological significance, the longer-lived NEP-evoked increase in $[Ca^{2+}]_i$ could cause a longer-lasting stimulation of Ca^{2+}- dependent exocytosis, i.e., have a greater secretory response than nicotinic receptor stimulation. Although experiments aimed at studying directly NEP-evoked exocytosis were not included under this AFOSR funded project, our participation in the AFOSR MURI on "Nanoelectropulse-Induced Electromechanical Signaling and Control of Biological Systems" (FA9550-15-1-0517) provided us with additional resources, namely a Master's student who was supported by the MURI project, to initiate these experiments. The strategy used was to visualize exocytotic events in real-time using TIRF microscopy, assessing both the number and time course of exocytotic events evoked in cells in response to 5 ns pulses versus those evoked by nicotinic receptor stimulation.

For these determinations, DMPP or 5 ns pulses were applied to chromaffin cells in which secretory granules were labeled with the fluorescent dye acridine orange. Figure 20 shows how exocytosis was then assessed. The top panel shows that a fluorescent secretory granule undergoing exocytosis releases its contents, causing a cloud of fluorescence. The loss of granule fluorescence in turn leaves an empty space. This sequence of events, which is well-described in the literature, is what we refer to as "classical-type" exocytosis, that is, the exocytosed granule is identifiable. In the second case (schematic in the lower panel), exocytosis was observed as a sudden cloud or "flash" of fluorescence that could not be traced to a visible secretory granule. This type of exocytosis we termed "flash" events to distinguish it from "classical-type" events.

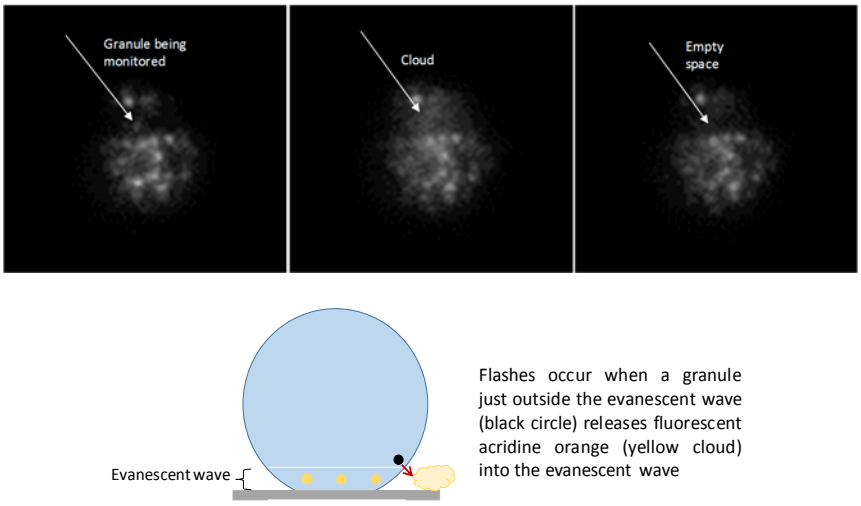

Figure 20. Exocytosis monitoring in chromaffin cells by TIRF microscopy. Secretory granules are stained with acridine orange and exposed to a stimulus. Top: Photomicrographs showing classical-type exocytosis in which a granule releases the fluorescent dye, causing an empty space. Bottom: Schematic depicting the nature of flash events.

The most significant of our findings are shown in Figure 21. When we compared the number of exocytotic events evoked by 10 applications of DMPP versus 10 pulses, we found first that the secretory response evoked by the NEPs was significantly greater relative to DMPP both in the number of events and the duration of the events. These results are consistent with the sustained increase in $[Ca^{2+}]_i$ that the NEP stimulus causes (refer to Figure 19). But we also found something quite unexpected. Despite the instantaneous rise in $[Ca^{2+}]_i$ evoked by the NEPs, exocytosis occurred after a delay of several seconds whereas exocytotic events triggered by DMPP were observed at the earliest recording time achievable with our imaging setup, 500 ms. The basis for the delay in NEP-evoked exocytosis is currently unknown and obviously important to pursue.

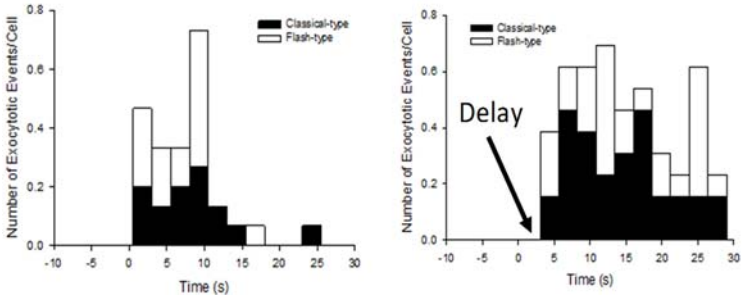

Figure 21. Comparison of exocytotic events evoked in chromaffin cells by 5 ns pulses versus a nicotinic receptor agonist. Secretory granules were labeled with acridine orange and the number of exocytotic events determined for 10 applications of DMPP (left) versus 10 pulses (right). Each stimulus train was applied at time zero.

4.7.1 Significance

Ca^{2+} entry via VGCCs is the trigger for exocytosis and a stimulus that evokes a prolonged increase in $[Ca^{2+}]_i$ via VGCCs should mean longer-lived exocytotic activity. This is indeed what we found. These results lead us to conclude that NEPs can serve as a very effective modality for neuromodulation.

4.8 Conditions for studying effects of NEPs on chromaffin cells in intact adrenal gland tissue are being established.

Isolated cell preparations are ideal for identifying fundamental mechanisms by which various types of stimuli affect cellular function and primary cultures of adrenal chromaffin cells will continue to serve as an important model cell system for elucidating effects of NEPs on cell excitability and neurosecretion. However, we recognize the need to investigate effects of NEPs on chromaffin cells also in a more physiological setting, which will provide a foundation for implementing NEPs to stimulate live excitable tissue *in vivo*. For this effort the strategy is to study the effects of NEPs on chromaffin cells in intact adrenal gland tissue, in particular, adrenal tissue from transgenic mice in which neural crest-derived adrenal medullary chromaffin cells are targeted to express specific genetically-encoded fluorescent reporters. These studies were undertaken with Dr. Thomas Gould in the Department of Physiology and Cell Biology.

In preliminary experiments, we took advantage of a transgenic mouse that drives expression of GCaMP3, a green fluorescent protein (GFP)-conjugated calmodulin, placed under the control of the Wnt1 promoter that limits expression of the protein to neural crest derivatives such as adrenal chromaffin cells. The advantage of GCaMP3 is that it fluoresces upon Ca^{2+} binding. As

shown in Figure 22, bath application of a nicotinic receptor agonist resulted in a robust Ca^{2+} response of the entire adrenal medulla, the location of chromaffin cells, in hemi-adrenal glands of *Wnt1-GCaMP3* mice; there was no increase in fluorescence in the outer adrenal cortex. To the best of our knowledge, we are the first group of researchers to demonstrate the ability to monitor Ca^{2+} dynamics in intact adrenal tissue in chromaffin cells expressing a Ca^{2+} reporter.

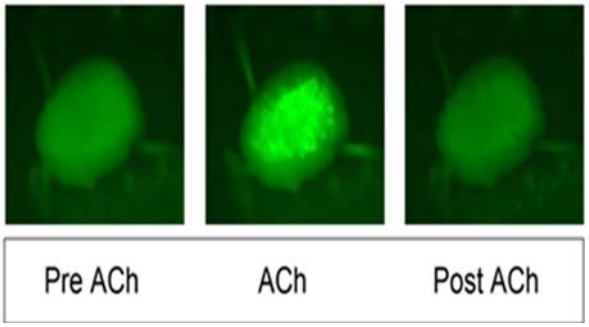

Figure 22. Chromaffin cells in the adrenal medulla express functional GCaMP3 in Wnt1-GCaMP3 mice that responds to Ca^{2+} influx evoked by a nicotinic receptor agonist. The hemi-adrenal gland of a Wnt1-GCaMP3 mouse was placed in a culture dish containing oxygenated Krebs and illuminated with a Spectra X light engine. Image sequences, which were captured using an Andor Neo sCMOS camera, show before (pre ACh), during (ACh) and after (Post ACh) bath application of the acetylcholine (ACh) receptor agonist carbachol that evokes Ca^{2+} influx in chromaffin cells that are located in the medulla, the inner portion portion of the adrenal gland.

We have also successfully isolated chromaffin cells from the adrenal glands of both wild-type mice and mice expressing the more sensitive GCaMP6f. Experiments have been initiated to compare the responses of wild-type versus GCaMP6f-expressing chromaffin cells to 5 ns pulses, as well as to compare the responses to bovine chromaffin cells.

5.0 CONCLUSIONS

During the 5-year award period our main accomplishments have been to characterize the plasma membrane mechanisms underlying NEP-evoked catecholamine release from isolated adrenal chromaffin cells. This characterization included elucidating effects on the lipid bilayer and on ion channels. In the process, we have uncovered several novel effects of NEPs, which need to be further explored to understand the mechanisms involved. Importantly, our studies do not provide evidence of adverse effects of NEPs that would question their potential for being developed into practical applications for modulating cell excitability.

Another accomplishment has been to determine that NEPs are a very effective stimulus for evoking exocytosis. To this end, we have made significant progress toward expanding our efforts to include NEP exposure of intact adrenal gland tissue. In collaboration with our colleagues at the AFRL in Fort Sam Houston, TX, we hope to be able to ultimately develop a device for warfighters to be used to stimulate the “fight or flight response” of the adrenal gland in times of need.

6.0 REFERENCES

1. Hassan, N., Chatterjee, I., Publicover, N.G., and Craviso, G.L., "Mapping membrane potential perturbations of chromaffin cells exposed to electric fields", *IEEE Transactions on Plasma Science* **30:**1516-1524, 2002.

2. Craviso, G.L., "Generation of functionally competent single bovine adrenal chromaffin cells using the neutral protease dispase", *Journal of Neuroscience Methods* **137**:275-281, 2004.

3. Craviso, G. L., Chatterjee, P., Maalouf, G., Cerjanic, A., Yoon, J., Chatterjee, I., and Vernier, P. T., "Nanosecond electric pulse-induced increase in intracellular calcium in adrenal chromaffin cells triggers calcium-dependent catecholamine release", *IEEE Transactions on Dielectrics and Electrical Insulation* **16**:1294-1301, 2009.

4. Craviso, G. L., Choe, S., Chatterjee, P., Chatterjee, I. and Vernier, P.T., "Nanosecond electric pulses: a novel stimulus for triggering Ca^{2+} influx into chromaffin cells via voltage-gated Ca^{2+} channels", *Cellular and Molecular Neurobiology* **30**:1259-1265, 2010.

5. Craviso, G.L., Choe, S., Chatterjee, I. and Vernier, P.T., "Modulation of intracellular Ca^{2+} levels in chromaffin cells by nanoelectropulses", *Bioelectrochemistry*, **87**:244-252, 2012 (epub 2011).

6. Zaklit, J., Craviso, G.L., Leblanc, N., Yang, L., Vernier, P.T., and Chatterjee, I., "Adrenal chromaffin cells exposed to 5-ns pulses require higher electric fields to porate intracellular membranes than the plasma membrane: an experimental and modeling study", *Journal of Membrane Biology*, **250:**535-552, 2017. doi: 10.1007/s00232-017-9983-9

7. Zaklit, J., Chatterjee, I., Leblanc, N., and Craviso, G.L., "Ultrashort nanosecond electric pulses evoke heterogeneous patterns of Ca^{2+} release from the endoplasmic reticulum of adrenal chromaffin cells", *Biochimica et Biophysica Acta-Biomembranes*, **1861:**1180-1188, 2019. doi: 10.1016/j.bbamem.2019.04.006

8. Yoon, J., Leblanc, N., Zaklit, J., Vernier, P.T., Chatterjee, I., and Craviso, G.L., "Enhanced monitoring of nanosecond electric pulse-evoked membrane conductance changes in whole-cell patch clamp experiments", *Journal of Membrane Biology*, **249**: 633-644**,** 2016. doi: 10.1007/s00232-016-9902-5

9. Smith, K.C., Weaver, J.C., "Active mechanisms are needed to describe cell responses to submicrosecond, megavolt-per-meter pulses: Cell models for ultrashort pulses", *Biophysical Journal*, **95**:1547-1563, 2008. doi: 10.1529/biophysj.107.121921

10. Neu, J.C., Krassowska, W., "Asymptotic model of electroporation", *Physical Review E*, 59:3471-3482, 1999. doi: 10.1103/PhysRevE.59.3471

11. Sabuncu, A.C., Stacey, M., Craviso, G.L., Semenova, N., Vernier, P.T., Leblanc, N., Chatterjee, I., and Zaklit, J., "Dielectric properties of isolated adrenal chromaffin cells determined by microfluidic impedance spectroscopy", *Bioelectrochemistry*, **119**:84-91, 2018. doi: 10.1016/j.bioelechem.2017.09.001

12. Smith, K.C., "Modeling cell and tissue electroporation", Master's thesis, *Dept. of Electrical Engineering and Computer Science, Massachusetts Institute of Technology*, Feb, 2006.

13. Pakhomov, A.G., Bowman, A.M., Ibey, B.L., Andre, F.M., Pakhomova O.N., and Schoenbach K.H., "Lipid Nanopores Can Form a Stable, Ion Channel-like Conduction Pathway in Cell Membrane", *Biochemical and Biophysical Research Communications*, **385**, **2**, Jul 2009, pp 181-186. doi:10.1016/j.bbrc.2009.05.035

14. Fenwick, E.M., Marty, A., and Neher, E., "Sodium and Calcium Channels in Bovine Chromaffin Cells", *Journal of Physiology*, **331:**599-635, 1982. doi: 10.1113/jphysiol.1982.sp014394

15. Marty, A., Neher, E., "Potassium Channels in Cultured Bovine Adrenal Chromaffin Cells", *Journal of Physiology*, **367**:117-147, 1985. doi:10.1113/jphysiol.1985.sp015817

16. Yang, L., Craviso, G.L., Vernier, P.T., Chatterjee, I., and Leblanc, N., "Nanosecond electric pulses differentially affect inward and outward currents in patch clamped adrenal chromaffin cells", *PLOSONE*, **12**, **7**, Jul 2017, e0181002. doi: 10.1371/journal.pone.0181002

PUBLICATIONS

1. Yoon, J., Leblanc, N., Zaklit, J., Vernier, PT., Chatterjee, I., and Craviso, GL., "Enhanced monitoring of nanosecond electric pulse-evoked membrane conductance changes in whole-cell patch clamp experiments", *Journal of Membrane Biology*, **249, 5**, Apr 2016, pp. 633-644. doi: 10.1007/s00232-016-9902-5

2. Zaklit, J., Craviso, G.L., Leblanc, N., Yang, L., Vernier, P.T., and Chatterjee, I., "Adrenal chromaffin cells exposed to 5-ns pulses require higher electric fields to porate intracellular membranes than the plasma membrane: an experimental and modeling study", *Journal of Membrane Biology*, **250:**535-552, 2017. doi: 10.1007/s00232-017-9983-9

3. Yang, L., Craviso, G.L., Vernier, P.T., Chatterjee, I., and Leblanc, N., "Nanosecond electric pulses differentially affect inward and outward currents in patch clamped adrenal chromaffin cells", *PLOSONE*, **12**, **7**, Jul 2017, e0181002. doi: 10.1371/journal.pone.0181002

4. Sabuncu, A.C., Stacey, M., Craviso, G.L., Semenova, N., Vernier, P.T., Leblanc, N., Chatterjee, I., and Zaklit, J., "Dielectric properties of isolated adrenal chromaffin cells determined by microfluidic impedance spectroscopy", *Bioelectrochemistry*, **119**:84-91, 2018. doi: 10.1016/j.bioelechem.2017.09.001

5. Bagalkot, T.R., Terhune, R.C., Leblanc, N., and Craviso, G.L., "Different membrane pathways mediate Ca^{2+} influx in adrenal chromaffin cells exposed to 150 - 400 ns electric pulses" , *BioMed Research International*. **2018**, 9046891. doi: 10.1155/2018/9046891.

6. Zaklit, J., Chatterjee, I., Leblanc, N., and Craviso, G.L., "Ultrashort nanosecond electric pulses evoke heterogeneous patterns of Ca^{2+} release from the endoplasmic reticulum of adrenal chromaffin cells", *Biochimica et Biophysica Acta-Biomembranes*, **1861:**1180-1188, 2019. doi: 10.1016/j.bbamem.2019.04.006

7. Bagalkot, T.R., Leblanc, N., and Craviso, G.L. "Stimulation or cancellation of Ca^{2+} influx by bipolar nanosecond pulsed electric fields in adrenal chromaffin cells can be achieved by tuning pulse waveform", *Scientific Reports*, **9**, Aug 2019, 11545. doi: 10.1038/s41598-019-47929-4

PRESENTATIONS

Conferences and meetings

Yoon, J., Leblanc, N., Pierce, S., Chatterjee, I., Vernier, P., Craviso, G.L., *Increase in chromaffin cell membrane conductance evoked by 5-ns electric pulses*. 36th Annual Bioelectromagnetics Society Meeting, Cape Town, South Africa, June 2014.

Yoon, J., Zaklit, J., Chatterjee, I., Vernier, P.T., Semenova, N., Leblanc, N., Craviso, G.L., *Transient versus sustained Ca^{2+} responses evoked in adrenal chromaffin cells by 5 ns pulses: pulse delivery considerations*. Annual BioEM Meeting, Asilomar, CA, June 2015.

Zaklit, J., Yoon, J., Chatterjee, I., Evans, E., Vernier, P.T., Leblanc, N., Craviso, G.L., *Ca^{2+} release from internal stores of adrenal chromaffin cells is not evoked by 5 ns electric pulses*. Annual BioEM, Asilomar, CA, June 2015.

Zaklit, J., Craviso G.L., Leblanc, N., Terhune, R., Chatterjee I., *Numerical modeling of intracellular adrenal chromaffin cell responses to high intensity 5 ns electric pulses*, Annual BioEM Meeting, Ghent, Belgium, June 2016.

Yang L., Craviso, G.L., Terhune, R., Vernier, P. T., Chatterjee, I., Leblanc N. *Potential differential effects of single high intensity 6 ns electric pulses on macroscopic inward and outward ionic currents recorded in whole-cell patch clamped bovine chromaffin cells*", Annual BioEM Meeting, Ghent, Belgium, June 2016.

Semenova N., Craviso G.L., Vernier P.T., *Nanosecond electric pulses cause a non-uniform increase of intracellular calcium concentration in adrenal chromaffin cells*", Annual BioEM Meeting, Ghent, Belgium, June 2016.

Yang, L., Leblanc, N., Vernier, P. T., Chatterjee, I. and Craviso, G.L., *Paradoxical effects of single and twin high intensity nanosecond electric pulses on inward Na^+ currents in bovine chromaffin cells*. 2nd World Congress on Electroporation and Pulsed Electric Fields in Biology, Medicine and Food & Environmental Technologies, Norfolk, VA, September 2017.

Shaw, A., Bagalkot, T., Sukhraj, R., Murray, K., Chatterjee, I., Leblanc, N., Craviso, G.L., *Real-time monitoring of chromaffin cell secretory granules by total internal reflection fluorescence microscopy reveals a stimulatory effect of nanosecond electric pulses (nsPEF) on exocytosis*. 2nd World Congress on Electroporation and Pulsed Electric Fields in Biology, Medicine and Food & Environmental Technologies, Norfolk, VA, September 2017.

Aramendia, G., Craviso, G.L., Leblanc, N., Zaklit, J., Burckhardt, K., Neufeld, E., Chatterjee I., *Detailed adrenal chromaffin cell model for studying the interaction of high intensity electric fields with membranes of secretory granules*. 2nd World Congress on Electroporation and Pulsed Electric Fields in Biology, Medicine and Food & Environmental Technologies, Norfolk, VA, September 2017.

Yang, L., Pierce, S., Vernier, P.T., Chatterjee, I., Craviso, G.L., Leblanc, N., *Differential effects of single and twin high intensity nanosecond electric pulses on membrane permeabilization and Na^+ conductance in adrenal chromaffin cells*. Annual Biophysical Society Meeting, San Francisco, CA, February 2018.

Yang, L., Pierce, S., Vernier, P. T., Chatterjee, I., Craviso, G.L., Leblanc, N. *Remarkable differences in the response of voltage-gated Na^+ current to a single or pair of high intensity nanosecond electric pulses in adrenal chromaffin cells*. Annual BioEM Meeting, Piran, Portorož, Slovenia, June 2018.

Sukhraj, R., Shoaf, A., Chatterjee, I., Leblanc, N., Craviso, G.L., *5 ns Electric pulses evoke Ca^{2+} responses in adrenal chromaffin cells that are longer in duration than those evoked by a physiological stimulus*. Annual BioEM meeting, Piran, Portorož, Slovenia, June 2018.

Zaklit, J., Chatterjee, I., Leblanc, N., Craviso, G.L. *High intensity, 5-ns electric pulses mobilize Ca^{2+} from two ER Ca^{2+} stores in adrenal chromaffin cells*. Biomedical Engineering Society Annual Meeting, Atlanta, GA, October 2018.

Yang, L., Pierce, S., Vernier, P.T., Chatterjee, I. Craviso, G.L., Leblanc, N. Differential effects of single and twin high intensity nanosecond electric pulses on membrane permeabilization and Na^+ conductance in adrenal chromaffin cells. Annual Biophysical Society Meeting, Baltimore, MD, March 2019

Zaklit, J., Craviso, G.L., Leblanc, N., Vernier, P.T., Sözer, E.B., *Electrostimulation of adrenal chromaffin cells by 2 ns electric pulses can be modulated by an electric field reversal.* Annual BioEM Meeting, Montpellier, France, June 2019.

Invited

Craviso, G.L., *Nanoelectropulse stimulation of neurosecretion*, International Scientific Workshop on Fundamental and Applied Bioelectrics, Frank Reidy Research Center for

Bioelectrics, Norfolk, VA, July 2014.

Craviso G.L., *Nanoelectropulse stimulation of neurosecretion*, Workshop on Fundamental & Applied Bioelectrics, Frank Reidy Research Center for Bioelectrics, Old Dominion University, Norfolk, VA, July 2016.

Craviso, G.L., "Nanoelectropulse stimulation of Neurosecretion". Workshop on Fundamental & Applied Bioelectrics, Norfolk, VA, July 2018.

Leblanc, N., "Deciphering and manipulating the properties of ion channels to modulate the function of excitable cells in health and disease". Frank Reidy Research Center for Bioelectrics, Old Dominion University, Norfolk, VA, January 2019.

POSTDOCTORAL FELLOWS

Jihwan Yoon, Ph.D., June 2014 to July 2015
Lisha Yang, Ph.D., September 2015 to present

STUDENT INVOLVEMENT

Graduate Students

Josette Zaklit, Ph.D. in Biomedical Engineering, December 2016.
Dissertation title: "Electroporation of intracellular membranes of adrenal chromaffin cells with high intensity, 5-ns electric pulses: an experimental and modeling study".

Guillermo Aramendia, M.S. in Electrical Engineering, August 2017.
Thesis title: "Asymmetrical transmembrane potential in intracellular organelles of adrenal chromaffin cells exposed to nanosecond electric pulses".

Ruby Sukhraj, M.S. in Biomedical Engineering, December 2019
Thesis title: **"**5 ns Electric pulses evoke a longer-lived calcium responses in adrenal chromaffin cells than those evoked by the physiological stimulus: an experimental and computational study".

Aaron Shaw (M.S. graduate student in Cellular and Molecular Biology) - research rotation carried out in fulfillment of a degree requirement

Undergraduate Students

1. **Research carried out in fulfillment of a degree requirement**
   Eric Evans (Biochemistry)
   Simon Li (Biochemistry)
   Jordanna Payne (Electrical Engineering)
   Adam Shoaf (Biochemistry)
   Ren Jensen (Biochemistry)
   Marissa Macedo (Biochemistry)

2. Student volunteers/lab aides

Marcelo de Carvalho Pereira (Electrical Engineering major)
Soo Hong Shin (Biochemistry major)
Nicole Zieba (Electrical Engineering major)
Hetvaben Patel (Neuroscience major)
Kyle Murray (Mathematics major)